Short Distance Position Control for Linear Switched Reluctance Motors: A Plug-in Robust Compensator Approach

Wai-Chuen Gan*, Norbert C. Cheung** and Li Qiu*
*Department of Electrical and Electronic Engineering, The Hong Kong University of Science and Technology, Clear Water Bay, Kowloon, Hong Kong SAR, China. Email: {eewcgan,eeqiu}@ee.ust.hk
**Department of Electrical Engineering, The Hong Kong Polytechnic University, Hung Hom, Kowloon, Hong Kong SAR, China. Email: eencheun@polyu.edu.hk

Abstract— **Short distance position control (< 1mm) is an important issue in many precision position applications such as integrated circuit (IC) bonding machines. For these purposes, a novel linear switched reluctance motor (LSRM) is developed. The motor's control strategy is based on a 20×20 look-up table force linearization scheme for low-cost implementation. The system performance is satisfactory for long and medium distance travels, but the system's output should be further improved for short ones. In this paper, a plug-in robust compensator is proposed to improve the tracking response of the overall system. Simulation and experimental results are presented and compared to validate the proposed robust plug-in compenstaor.**

I. Introduction

Short distance position control (< 1mm) is an important issue in precision position applications such as integrated circuit (IC) bonding machines. Switched reluctance motor has never been a popular choice for high precision and high speed motion actuator because the motor characteristic is highly dependent on its complex magnetic circuit, which is difficult to model, simulate, and control. However, there are increasing research on the switch reluctance motors [1] due to the advancement of power electronics and digital signal processors, as well as the sophisticated control algorithms.

In this paper, a novel linear switched reluctance motor (LSRM) was developed for precision manufacturing automation. The control strategy is based on a simple but effective look-up table force linearization scheme for low-cost implementation. The system performance is good for long and medium distance travels, but the system's output should be improved for short ones [2]. In this paper a plug-in robust compensator is proposed to improve the tracking response for the overall system. The proposed compensator improves the system performance when there are parameter variations in the system plant, or when the plant nonlinearity cannot be compensated exactly by the existing controller. The $\mathcal{H}_\infty$ loop shaping optimization technique is employed for the design of the robust compensator and the implementation of the proposed controller is simple and suitable for low-cost application.

The paper organization is as follows. The construction and the modeling of the LSRM are reviewed in Section II. Then, the existing look-up table force linearization control strategy is introduced and the problem for short distance position control is addressed in Section III. The proposed robust compensator is introduced in Section IV to enhance the system robustness and improve the tracking performance. In Section V, simulation and experimental results are presented and compared to validate the proposed compensator. Concluding remarks are given in Section VI.

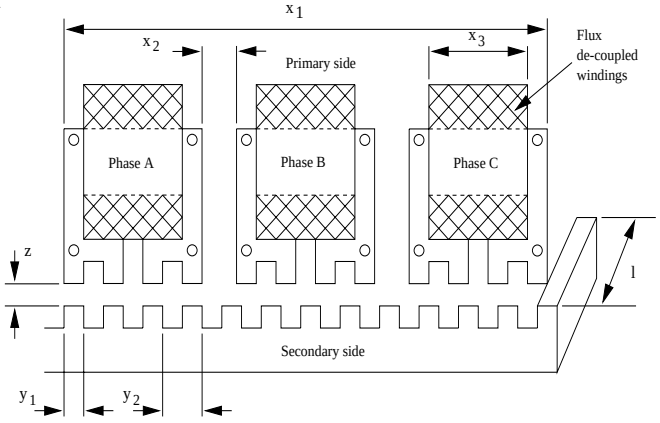

Fig. 1. Design schematic of the LSRM.

II. Construction and Modeling of the LSRM

The novel actuator design is based on switched reluctance technology [3]. The magnet-free structure makes this actuator particularly suitable for harsh environment such as high temperature and high pressure, etc. The flux de-coupled rotor arrangement leads a more simple motor model because there are no mutual inductances between windings [4]. Fig. 1 shows the design schematic of the LSRM system while Fig. 2 shows the prototype. The actuator is optimized for (i) high power-to-size ratio, (ii) low force ripple, (iii) low leakage and eddy current loss, and (iv) fast current dynamics.

The motor is integrated on a precision linear motion guide. A linear optical encoder with 0.5um accuracy is mounted on the motion actuator to observe the motion profile and provides the position feedback. In addition, the tracking guide and the core of the windings are laminated with 0.5mm silicon-steel plates. Table I shows the characteristics of the proposed LSRM.

The switched reluctance linear drive system has a highly nonlinear characteristic due its nonlinear flux behavior [6].

0-7803-7116-X/01/$10.00 (C) 2001 IEEE

TABLE I

LSRM CHARACTERISTIC

Power output	100W
Traveling distance	300mm
Maximum load	5kg
Pole width	5mm (y_1)
Pole pitch	10mm (y_2)
Coil separation	8.333mm (x_2)
Winding width	15mm (x_3)
Air gap width	0.4mm (z)
Track width	25mm (l)
Aligned phase inductance	19.8mH
Unaligned phase inductance	11.4mH
Feedback device	Optical encoder 0.5μm resolution

Following is the mathematical model of the LSRM:

$$v_j = R_j i_j + \frac{\partial \lambda_j(x,i_j)}{\partial x}\frac{dx}{dt} + \frac{\partial \lambda_j(x,i_j)}{\partial i_j}\frac{di_j}{dt} \quad (1)$$

$$f_e = \sum_{j=1}^{3} \frac{\partial \int_0^{i_j} \lambda_j(x,i_j) di_j}{\partial x} \quad (2)$$

$$f_e = M_m \frac{d^2x}{dt^2} + B_m \frac{dx}{dt} + f_l \quad (3)$$

where v_j, i_j, R_j and λ_j are the phase voltage, phase current, phase resistance and phase flux linkage respectively, x is the travel distance, f_e is the generated electromechanical force, f_l is the external load force, M_m and B_m are the mass and the friction constants respectively.

The proposed LSRM has the unique open structure so that the force-current-position characterization chart can be measured experimentally without great difficulty. Fig. 3 shows the measurement results for a single phase motor winding. The experimental data are stored in a 20×20 look-up table for the implementation of the force linearization scheme which will be described in Section III.

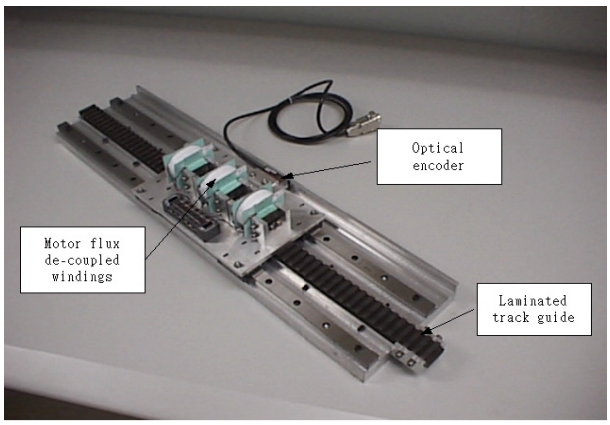

Fig. 2. The prototype.

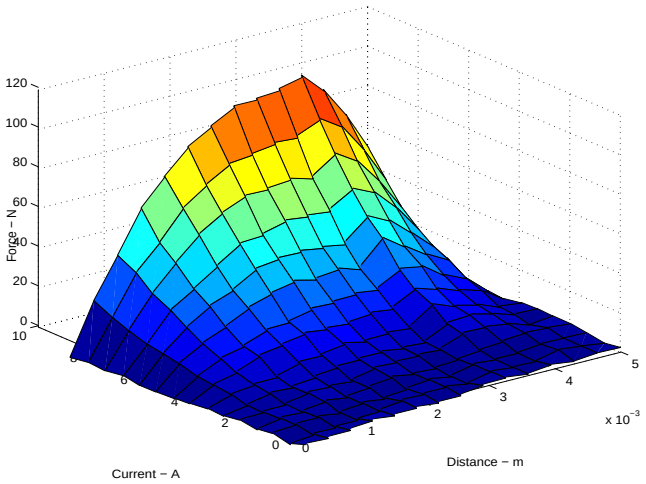

Fig. 3. 3D force-current-position plot.

III. Problem for Short Distance Position Control

The central part in our LSRM controller is the look-up table force linearization scheme. Although there are many sophisticated torque linearization control algorithms for switched reluctance motors [7], [8], their computational complexity is too demanding so that they are not suitable for low-cost implementation. On the other hand, look-up table is found to be a simple but effective force linearization scheme [9] and can easily be implemented on a low-cost fixed-point micro-controller.

In this project, a small look-up table, (20×20) elements, is employed to store the force compensation values. Two-dimensional linear interpolation is used to find the intermediate values. Fig. 4 shows the method of obtaining the required current i^* by bi-linear interpolation. Firstly, from the position x_{in} and force F_{in} inputs, two pairs of data in the look-up table $i_{(F_1,x_1)}$, $i_{(F_2,x_1)}$ and $i_{(F_1,x_2)}$, $i_{(F_2,x_2)}$ are located. For each pair, a linear interpolation is done, according to the ratio of F_1, F_2, and F_{in}. As a result two intermediate elements $i_{(F_{1-2},x_1)}$ and $i_{(F_{1-2},x_1)}$ are obtained. Finally, the output current command i^* is obtained by interpolating the two intermediate elements with x_1, x_2, and x_{in}.

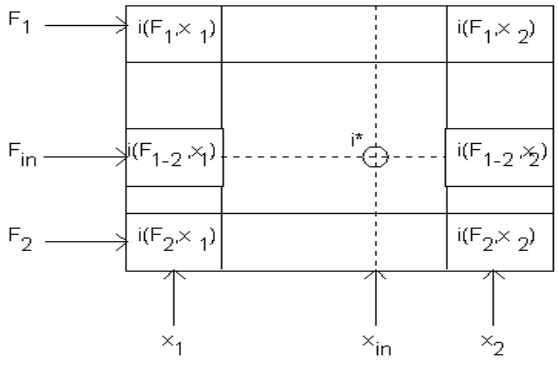

Fig. 4. Calculating i^* from the look-up table

The standard two degree of freedom (2DOF) motion controller is adopted for the position control. Fig. 5 shows the overall motor controller including the look-up table force linearization scheme. In general, the 2DOF controller $[\ C_1 \quad -C_2\ ]$ can be any controllers which can stabilize the overall system and ensure a desirable closed-loop frequency response. In this particular example, $C_2 = \frac{c_{20}s+c_{21}}{\delta_1 s+1}$ with $\delta_1 > 0$ is chosen, which is basically a PD controller with a low-pass filter in the differentiation term. The feedforward controller is chosen as $C_1 = \frac{c_{10}s+c_{11}}{\delta_1 s+1}$.

By using the existing controller structure, the tracking responses for long and medium travels are good and the results were reported in [2]. However, the tracking response should be improved for the short distance travel ($<$ 1mm). Fig. 6 shows the experimental results for a 250um travel. Nonlinear effect, poor transient tracking and overshoot are observed.

For a such short distance travel, the required force is very small so that the force look-up table is not capable of compensating the nonlinearity in this particular region. To verify our claim, the force loop is extracted alone and tested by simulation. Fig. 7 shows the force tracking response for long distance travel and the input force reference is derived from the 3rd order S-profile. The tracking response is good for long distance travel and this explains why we can obtain desirable results in [2]. Fig. 8 shows the force tracking response when the input force reference is for a short distance travel (250um). Obviously, the look-up table scheme fails to compensate the nonlinearity for this small region and hence an unacceptable results are obtained as shown in Fig. 6.

The poor transient response for short distance travels comes from the imperfect linearization compensation and there are three possible solutions to solve this problem. Namely, (i) enlarging the size of the look-up table, (ii) applying adaptive control or nonlinear control for exact force linearization, (iii) applying plug-in robust control to take care the model uncertainty for short distance travel. The first two are not optimal solutions for low-cost implementation due to the low computational power and small memory space for an economical fixed-point micro-controller. However, low-cost micro-controllers are still capable of implementing fixed-order robust controller as the one we design in the next section.

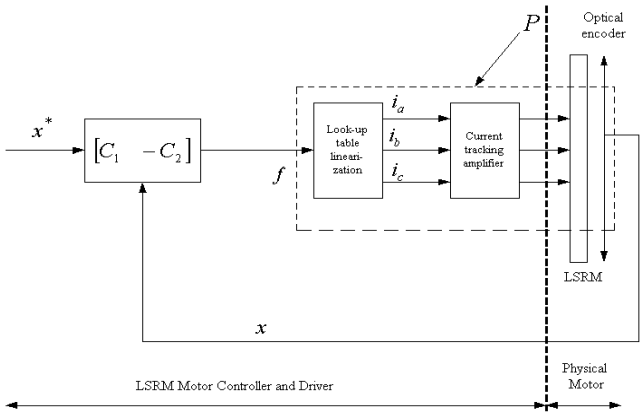

Fig. 5. Overall controller structure

IV. Design of the Plug-in Robust Compensator

The controller C described in the previous section can achieve satisfactory tracking performance for medium and long distance travels but not for short distance travels. Therefore, an effective way to solve the above problem is to design a robust plug-in compensator which can serve the following purposes. Firstly, the tracking performance for short distance travel should be enhanced by using this compensator. Secondly, the proposed compensator can be co-exist with the existing controller C and without deteriorating the tracking response for medium and long distance travels. Finally, the system stability of the overall system should still be guaranteed after adding the plug-in robust compensator.

Consider the feedback system shown in Fig. 9. Assume P is an SISO strictly proper nominal system. In our LSRM system, the nominal plant is equal to $P = P_0 = \frac{1}{s(M_m s+B_m)}$, r is the reference command position x^*, and y is the controlled position output x. Initially assume that the two degree of freedom (2DOF) controller $K = [\ K_1 \quad -K_2\ ]$ is given by $K = C = [\ C_1 \quad -C_2\ ]$ which is the existing controller that we employed in the previous section with satisfactory nominal tracking performance for medium and long travel distances, i.e. the transfer function from reference r to output y

$$\frac{Y}{R} = \frac{C_1 P}{1 + C_2 P}$$

is satisfactory.

Let a coprime factorization of P be given as

$$P = \frac{N}{M}$$

where $M,\ N \in \mathcal{H}_\infty$. Since C is a stabilizing 2DOF con-

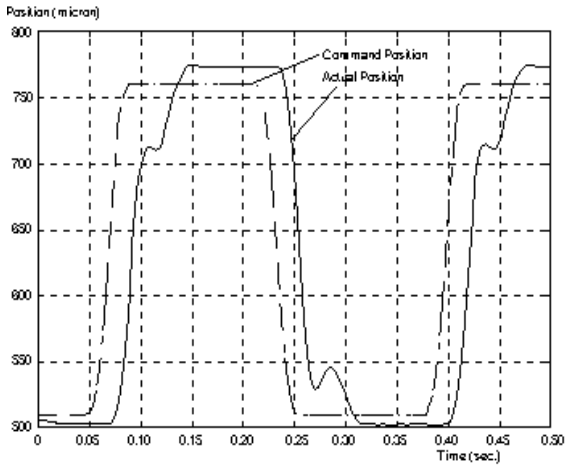

Fig. 6. Transient response for short distance travel (250um)

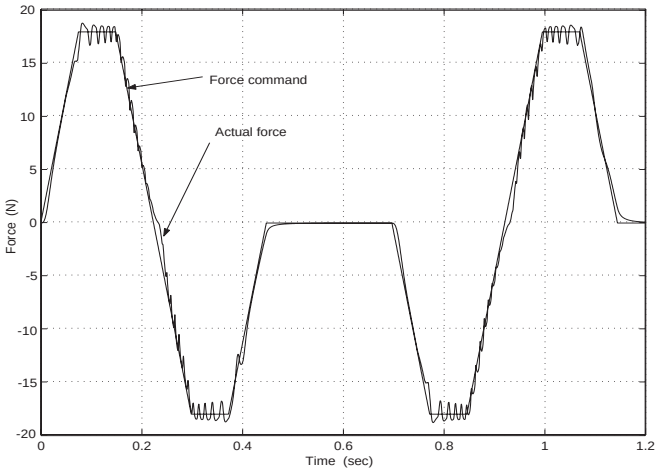

Fig. 7. Force tracking for long/medium travel distance.

troller for P, for any coprime factorization

$$C = \frac{[\ X_1 \quad -X_2\ ]}{Y_0}$$

where X_1, X_2 and $Y_0 \in \mathcal{H}_\infty$. It is shown in [10], Theorem 15 of Section 5.6, that all 2DOF stabilizing controller can be parameterized as

$$[\ K_1 \quad -K_2\ ] = \frac{[\ S \quad -(X_2 + QM)\ ]}{(Y_0 - QN)} \tag{4}$$

where $Q \in \mathcal{H}_\infty$ and $S \in \mathcal{H}_\infty$ are arbitrary systems. If we plug $K = [\ K_1 \quad -K_2\ ]$ to the feedback system, then the transfer function from r to y becomes

$$\frac{Y}{R} = \frac{NS}{Y_0 M - X_2 N}$$

which is independent of Q. Since we are satisfied with the original transfer function from r to y when $C = [\ C_1 \quad -C_2\ ]$ is used, it then follows that we can choose $S = X_1$ since

$$\frac{Y}{R} = \frac{NS}{Y_0 M - X_2 N} = \frac{C_1 P}{1 + C_2 P} = \frac{N X_1}{Y_0 M - X_2 N}.$$

Therefore, the set of all stabilizing 2DOF controller which gives the same nominal tracking performance is given by

$$[\ K_1 \quad -K_2\ ] = \frac{[\ X_1 \quad -(X_2 + QM)\ ]}{(Y_0 - QN)}.$$

The loop property of the feedback system, which depends on K_2 and P only, now depends on Q only. For any stable system Q, which can even be nonlinear and time varying, the nominal tracking performance is unaffected and the closed loop stability is guaranteed [13], [14]. Suppose that a Q is chosen, theoretically there are two ways to implement the new controller K. One is to explictly obtain K from (4) and implement as in Fig. 9. The other way is to use the structure in Fig. 10. Clearly, the first way requires the dismantling of the original controller $C = [\ C_1 \quad -C_2\ ]$. It is the use of the structure in Fig. 10 that gives us the plug-in feature of our additional controller. Now we give one method to design a Q for enhancing the robustness of the control system.

A. $\mathcal{H}_\infty$ Loop Shaping Plug-in Controller Design

Since the purpose of Q is to improve the loop property of the feedback system, the tracking issue is not of concern in its design. The feedback loop part of the whole system is redrawn in Fig. 11 with the reference injection part ignored. Fig. 11 can be simplified to Fig. 12 with $K_2 = \frac{X_2 + QM}{Y_0 - QN}$. Our idea in the design of a stable Q is to design a stabilizing K_2 and then back substitute to get Q using

$$Q = \frac{K_2 Y_0 - X_2}{M + K_2 N} \tag{5}$$

which is obtained from (4). Since all stabilizing K_2 are obtained from

$$K_2 = \frac{X_2 + QM}{Y_0 - QN}$$

over all stable Q, it follows that Q obtained from (5) for a stabilizing K_2 has to be stable.

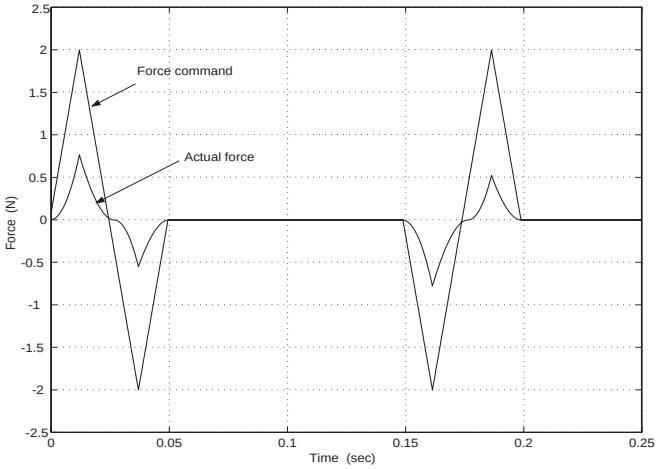

Fig. 8. Force tracking for short distance travel (20×20 look-up table).

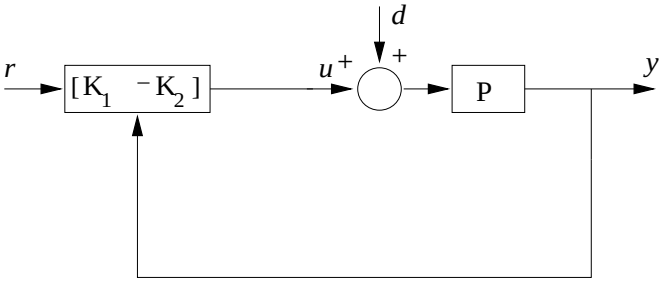

Fig. 9. General 2DOF controller.

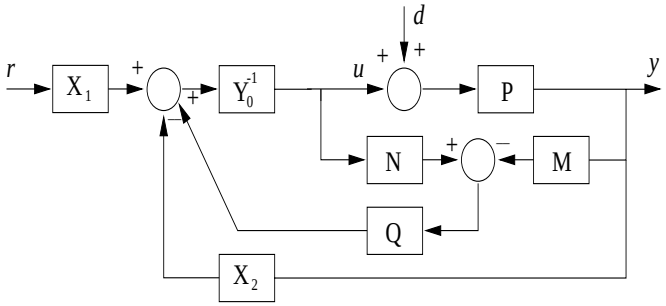

Fig. 10. Proposed plug-in robust compensator.

The $\mathcal{H}_\infty$ loop shaping design [11] is employed to design the stabilizing controller K_2 in Fig. 12. The control problem is to design the block Q so that the following $\mathcal{H}_\infty$ norm can be optimized:

$$\left\| \begin{bmatrix} I \\ K_3 \end{bmatrix} (I + P_s K_3)^{-1} \begin{bmatrix} I & P_s \end{bmatrix} \right\|_\infty \tag{6}$$

where $P_s = W_1 P W_2$ is the shaped plant, W_1 and W_2 are pre-/post-filters and K_3 is the $\mathcal{H}_\infty$ controller. The design of the controller K_2 is further divided into two steps. The first step is to choose a proper pre-filter W_1 and post-filter W_2 so that the shaped plant, $P_s = W_1 P W_2$, has a desired open loop frequency response according to some well-defined specifications such as bandwidth or steady state error requirement. Then the $\mathcal{H}_\infty$ controller K_3 can be found by using the solution in [11] or the command *ncfsyn* of MATLAB μ-Analysis and Synthesis Toolbox [12]. The controller K_2 is implemented by combining the pre-filters W_1, W_2 and the $\mathcal{H}_\infty$ controller K_3 as $K_2 = W_1 K_3 W_2$. Fig. 13 shows the $\mathcal{H}_\infty$ loop shaping controller design procedure. Finally, the block Q can be found in (5).

Since our plant is a SISO strictly proper unstable system, it follows that $N = \frac{1}{(\delta_2 s+1)(M_m s+B_m)}$ and $M = \frac{s}{(\delta_2 s+1)}$ can be assigned and δ_2 is any positive constant. Now the problem is reduced to the choices of proper pre-filter and post-filter. As our plant is a SISO system, we can simply assign $W_2 = 1$ and only put emphasis on the choice of W_1. The systematic design procedure of the filter W_1 is as follows. Firstly, to minimize the order of the final controller, the inverse of the stable mode of the nominal plant $(M_m s + B_m)$ is included in W_1. Secondly, instead of eliminating a constant disturbance, a ramp disturbance is expected to be rejected by our proposed controller; therefore, an integrator should be placed from y to u in Fig. 12 because our plant is a type 1 system. Hence, the simplest choice of W_1 is equal to $\frac{\alpha(M_m s+B_m)}{s}$ where α is a constant used to adjust the bandwidth of the shaped plant.

The main advantage of $\mathcal{H}_\infty$ loop shaping controller over $\mathcal{H}_\infty$ mixed-sensitivity controller is that the selection of the weighting functions, which is very difficult to assign properly in practice, is unnecessary in the design process. Instead, pre-filter and post-filter are used to shape the open loop plant to achieve a desired frequency response according to some well defined design specifications such as bandwidth, and steady state error, etc. Furthermore, the $\mathcal{H}_\infty$ norm in (6) actually includes the balance of the sensitivity and complementary functions as the design objective in the $\mathcal{H}_\infty$ mixed-sensitivity optimization. Therefore, $\mathcal{H}_\infty$ loop shaping controller can perform or outperform what $\mathcal{H}_\infty$ mixed-sensitivity controller can do by choosing W_1 and W_2 properly.

V. Simulation and Experimental Results

Without the plug-in robust compensator, the existing controller C and the nominal plant are equal to:

$$C_1 = \frac{4500s+1000}{0.001s+1} \quad C_2 = \frac{5000s+1000}{0.001s+1} \quad P = P_0 = \frac{1}{s(1.2s+0.08)}.$$

It follows that the coprime factorization of P be given as

$$N = \frac{1}{(0.001s+1)(1.2s+0.08)} \quad M = \frac{s}{(0.001s+1)}.$$

For the design of the block Q, $Y_0 = \frac{0.001s+1}{5000s+1000}$, $X_1 = \frac{4500s+1000}{5000s+1000}$, $X_2 = 1$, are first assumed, then the pre-filter is assigned as $W_1 = \frac{10^6(1.2s+0.08)}{s}$. The shaped plant $P_s = \frac{10^6}{s^2}$ is resulted and its bode plot is shown in Fig. 14. Following the solution in [11], the $\mathcal{H}_\infty$ controller, $K_3 = \frac{2.414(s+414.21)}{(s+2.41\times10^3)}$, is a first order stable transfer function. Then from (5), the final solution Q is equal to

$$Q = \frac{-4.2\times10^{-4}(s+3.93\times10^3)(s+1000)(s-145.08)(s+0.0668)}{(s^2+1416.9s+1.0069\times10^6)(s+993.1)(s+0.2)}.$$

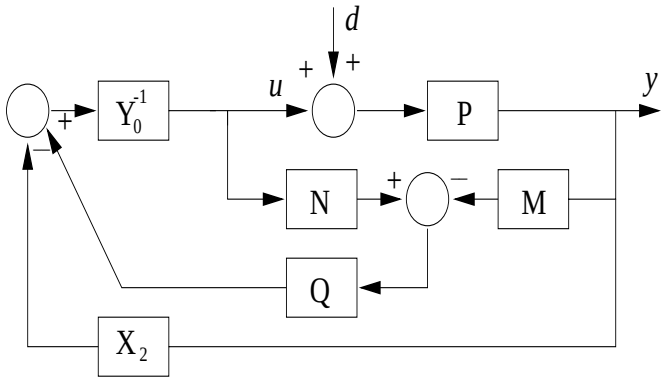

Fig. 11. Block digram for the design of the plug-in compensator Q.

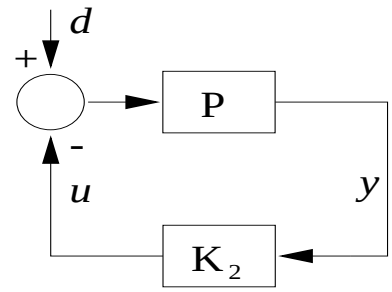

Fig. 12. Standard feedback configuration.

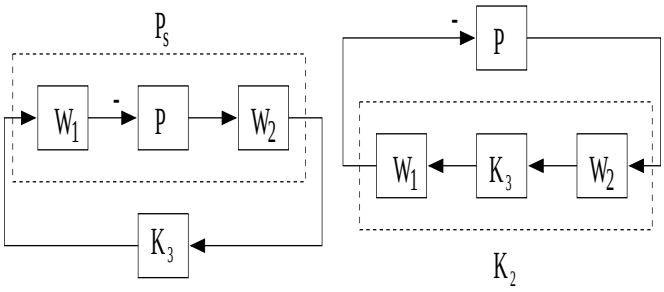

Fig. 13. $\mathcal{H}_\infty$ loop shaping controller design procedure.

The motor model, simple existing controller C and the plug-in robust compensator are embedded in MATLAB/SIMULINK for simulation purpose. The test input reference is a 250μm third-order position profile. Fig. 15 shows the tracking response when the plug-in compensator is turned off. It can be seen that there are overshoot, nonlinearity and steady state error present. With the help of the plug-in robust compensator, the new tracking response is depicted in Fig. 16. The nonlinearity can be compensated and the steady state error can also be eliminated.

Practical experiments are further performed to test the proposed plug-in compensator. Fig. 17 shows the experimental setup at the power electronics laboratory in the Hong Kong Polytechnic University. A dSPACE DS1102 control board is plugged into an ISA bus of a Pentium II computer and performs all the control functions. For the current tracking amplifier, three asymmetric bridge IGBT inverters are employed to drive the LSRM. Since the pulse width modulation driver needs to have a chopping frequency that is substantially higher than the current loop bandwidth, a chopping frequency of 12.5kHz is selected. A voltage of 90V is employed to supply the three asymmetric bridges. Note that the present setup is intended for development purpose only. The proposed control scheme can be implemented on a low-cost digital signal processor or even on a micro-controller.

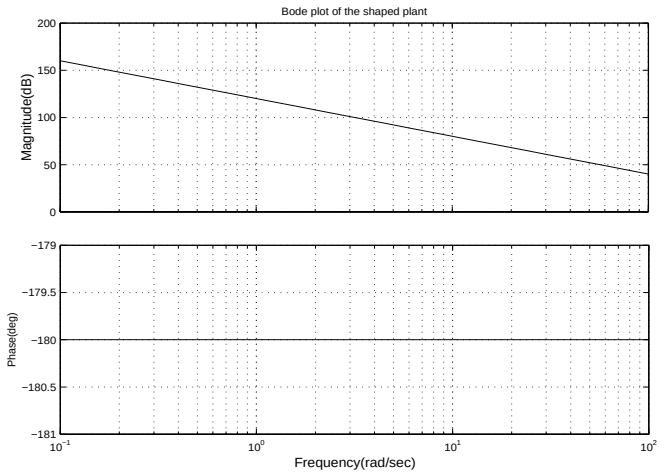

Fig. 14. Bode plot of the shaped plant $P_s = W_1 P$.

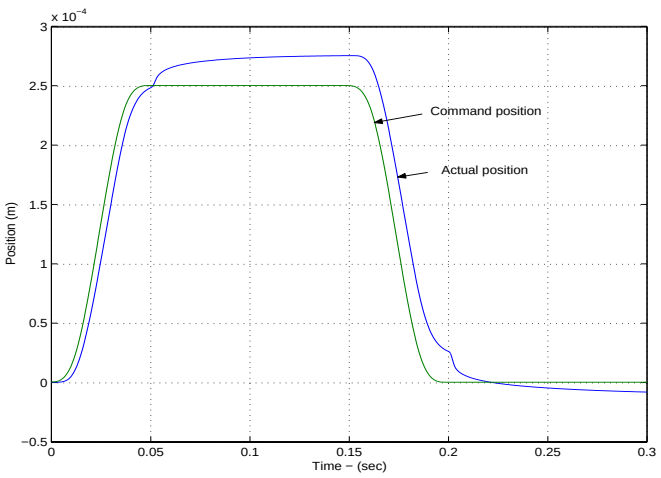

Fig. 15. Position tracking for 250um travel (without plug-in compensator).

The closed-loop position tracking is investigated with a 250um short distance travel reference, Fig. 18 depicts the position tracking response and it can be seen that the nonlinearity and overshoot can be eliminated. Although the steady state error (3μm) still exists for the return journey, the performance is greatly enhanced in comparison to the one without the plug-in compenstaor as shown Fig. 6. Fig. 19 shows the force command signal and the actual current for the phase A motor winding. The long distance position tracking response is shown in Fig. 20 with the plug-in robust compensator, the performance is still as good as before with improvement in the steady state error. This proves the plug-in compensator does not affect the tracking response gained by the nominal controller C.

In summary, the simulation and experimental results matched very well and this validates the proposed plug-in robust compensator can improve the system performance for short distance travels in a LSRM system.

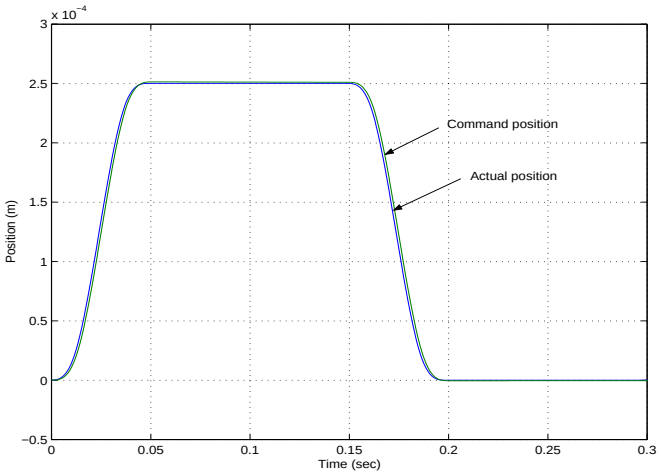

Fig. 16. Position tracking for 250um travel (with plug-in compensator).

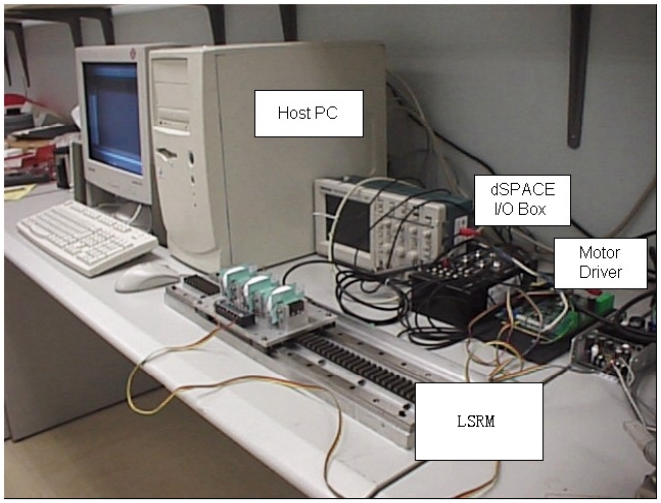

Fig. 17. Experimental setup in HKPU.

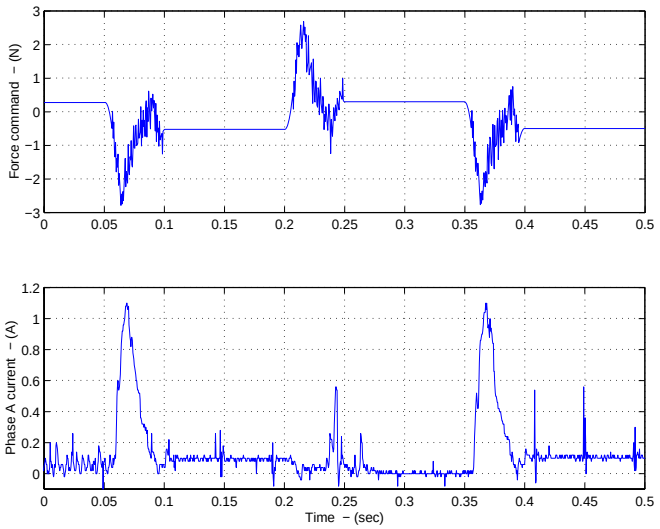

Fig. 19. Force command and actual current for phase A.

VI. Conclusions

Short distance position control for linear motor is very important for precision application. The look-up table force linearization is not capable of compensating the non-linearity for short distance travel (< 1mm). In this paper, a plug-in robust compensator is proposed to solve the problem. Following the systematic design procedure, a static plug-in robust controller is resulted and can be implemented easily by using low-cost digital signal processors or micro-controllers. From the simulation and experimental results, the position tracking response is found to be improved by using the plug-in compensator. With the plug-in robust compensator, both the long and short distance travels can be tracked accurately and hence the proposed low-cost LSRM system can be applied to many new and high-end applications which require high precision and high speed motion. It will also have a tendency to replace many traditional X-Y tables that operated by rotary motors and mechanical lead screws.

Acknowledgment

The authors would like to thank the Research Grants Council for the funding of this research work through the Competitive Earmarked Research grant PolyU5100/99E.

References

[1] T. J. E. Miller, *Switched Reluctance Motor and Their Control*, Magne Physics Publishing and Clarendon Press, Oxford, 1993.

[2] N. C. Cheung, "A robust and low-cost linear motion system for precision manufacturing automation," *IEEE Industry Applications Society 35th Annual Meeting*, vol. 1, pp. 40-45, Oct. 2000.

[3] I. Boldea, *Linear electric actuators and generators*, Cambridge University Press, 1997.

[4] W. C. Gan and N. C. Cheung, "Design of a linear switched reluc-

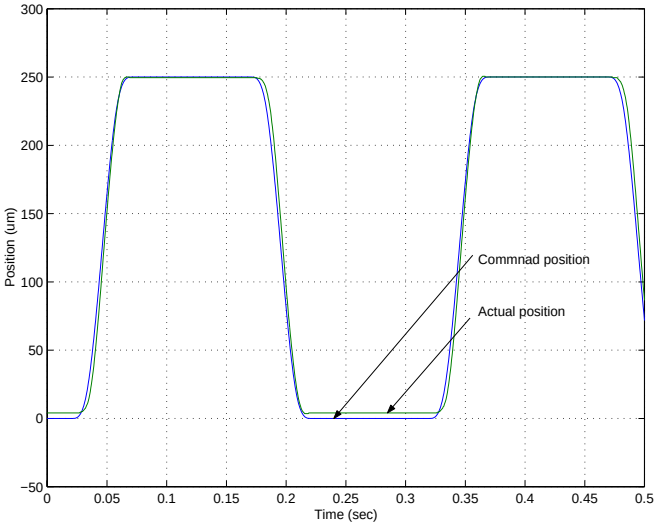

Fig. 18. Experimental position tracking for 250um travel (with plug-in compensator).

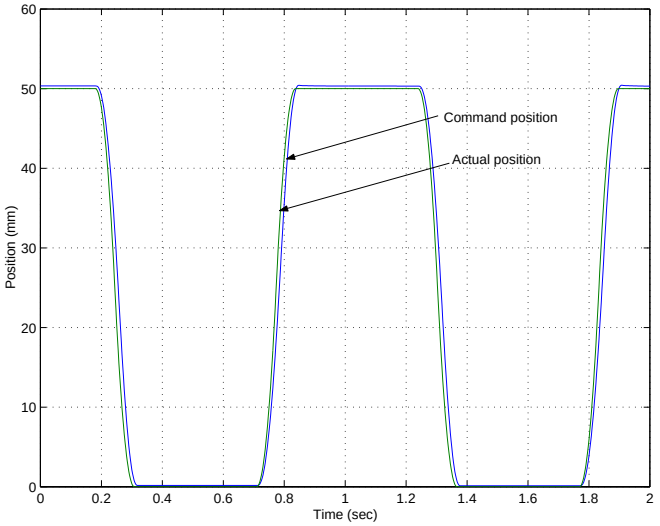

Fig. 20. Experimental position tracking for 50mm travel (with plug-in compensator).

tance motor for high precision applications," *IEEE International Electric Machines and Drives Conference*, Jun. 2001.
[5] F. Filicori, C. G. L. Bianco and A. Tonielli, "Modeling and control strategies for a variable reluctance direct-drive motor," *IEEE Trans. on Industrial Electronics*, vol. 40, no. 1, pp. 105-115, Feb. 1997.
[6] M. F. Rahman, N. C. Cheung and K. W. Lim, "Modelling of a nonlinear solenoid towards the development of a proportional actuator," *Proc. of the 5th International Conference on Modelling and Simulation of Electrical Machines Convertors and Systems*, ELECTRIMACS'96, Saint Nazaire, France, vol. 2, pp.695-670, Sep. 1996.
[7] P. C. Kjaer, J. J. Gribble and T. J. E. Miller, "High-grade control of switched reluctance machines," *IEEE Trans. on Industrial Electronics*, vol. 33, no. 6, pp. 1585-1593, Nov. 1997.
[8] H. K. Bae, B. S. Lee, P. Vijayraghavan and R. Krishnan, "A linear switched reluctance motor: converter and control," *IEEE Trans. on Industrial Applications*, vol. 36, no. 5, pp.1351-1359, Sept. 2000.
[9] M. F. Rahman, N. C. Cheung and K. W. Lim, "Converting a switching solenoid to a proportional actuator," *Trans. of IEE Japan*, vol. I16, pt. D, no. 5, pp.531-537, May 1996.
[10] M. Vidyasagar, *Control System Synthesis*, The MIT Press, Cambridge, 1985.
[11] D. C. McFarlane and K. Glover, *Robust Controller Design Using Normalized Coprime Factor Plant Descriptions*, Springer-Verlag, 1990.
[12] G. J. Balas, J. C. Doyle, K. Glover, A. Packard and R. Simth, *μ-Analysis and Synthesis Toolbox*, Mathworks Inc., 1994.
[13] K. Zhou, "A new controller architecture for high performance, robust, adaptive, and fault tolerant control," *Proceedings of the 39th IEEE Conference on Decision and Control*, vol. 4, pp. 4120-4125, 2000.
[14] P. P. Khargonekar and K. R. Poolla, "Uniformally optimal control of linear time-invariant plants: nonlinear time-varying controllers,"